land

MDPI

Article

Long Time-Series Monitoring and Drivers of Eco-Quality in the Upper-Middle Fen River Basin of the Eastern Loess Plateau: An Analysis Based on a Remote Sensing Ecological Index and Google Earth Engine

Yanan He [1], Baoying Ye [1,2], Juan He [1], Hongyu Wang [1] and Wei Zhou [1,2,3,*]

[1] School of Land Science and Technology, China University of Geosciences, Beijing 100083, China; 2112220084@email.cugb.edu.cn (Y.H.)
[2] Key Laboratory of Land Consolidation and Rehabilitation, Ministry of Natural Resources, Beijing 100083, China
[3] Technology Innovation Center for Ecological Restoration in Mining Areas, Ministry of Natural Resources, Beijing 100083, China
* Correspondence: zhouw@cugb.edu.cn

Abstract: Healthy watershed environments are essential for socioeconomic sustainability. The long-term monitoring and assessment of watershed ecological environments provide a timely and accurate understanding of ecosystem dynamics, informing industry and policy adjustments. This study focused on the upper-middle Fen River Basin (UMFRB) in eastern China's Loess Plateau and analyzed the long-term spatial and temporal characteristics of eco-quality from 2000 to 2023 by calculating a remote sensing ecological index (RSEI) via the Google Earth Engine (GEE) platform. In addition, this study also explored the trends and future consistency of the RSEI, as well as the impacts of natural and anthropogenic factors on RSEI spatial variations. The findings revealed that (1) the average RSEI value increased from 0.51 to 0.57 over the past 24 years, reflecting an overall improvement in eco-quality, although urban centers in the Taiyuan Basin exhibited localized degradation. (2) The Hurst index value was 0.468, indicating anti-consistency, with most regions showing trends of future decline or exhibiting stochastic fluctuations. (3) Elevation, temperature, precipitation, slope, and land use intensity are significantly correlated with ecological quality. Natural factors dominate in densely vegetated regions, whereas socioeconomic factors dominate in populated plains. These results provide valuable guidance for formulating targeted ecological restoration measures, protection policies, and engineering solutions.

Keywords: upper-middle Fen River Basin; ecosystem environment quality; remote sensing ecological index; Google Earth Engine; driving factors; geographically weighted regression

check for updates

Citation: He, Y.; Ye, B.; He, J.; Wang, H.; Zhou, W. Long Time-Series Monitoring and Drivers of Eco-Quality in the Upper-Middle Fen River Basin of the Eastern Loess Plateau: An Analysis Based on a Remote Sensing Ecological Index and Google Earth Engine. *Land* **2024**, *13*, 2239. https://doi.org/10.3390/land13122239

Academic Editor: Dong Jiang

Received: 5 November 2024
Revised: 17 December 2024
Accepted: 18 December 2024
Published: 20 December 2024

Copyright: © 2024 by the authors. Licensee MDPI, Basel, Switzerland. This article is an open access article distributed under the terms and conditions of the Creative Commons Attribution (CC BY) license (https://creativecommons.org/licenses/by/4.0/).

1. Introduction

Watersheds are among the most critical ecosystems on Earth and offer substantial ecological value [1]. These ecosystems provide the essential water resources, food, and favorable climatic conditions necessary for the survival of diverse species, thereby functioning as habitats for countless organisms. Additionally, the water cycle within watersheds regulates the climate and plays a crucial role in soil conservation, flood prevention, and disaster preparedness [2]. However, excessive human activities—such as urbanization [3], industrial wastewater discharge [4], overcultivation [5], overirrigation [6], dam construction [7], and water diversion [8]—have caused severe ecological issues in many watersheds worldwide, including extensive soil erosion, vegetation degradation, and water quality decline. In response, the Chinese government has implemented comprehensive watershed management plans; established water ecosystem and environmental management systems; and promoted various ecological restoration projects, including small-watershed

management and the integrated management of mountains, waters, forests, farmlands, lakes, grasslands, and deserts [9]. Within this context, the continuous monitoring and accurate assessment of watershed ecological quality are essential for formulating targeted environmental protection policies and achieving sustainable development goals.

Remote sensing technology, renowned for its broad coverage, rapid data acquisition, and cost-effectiveness features [10], has become increasingly prevalent in ecological environment monitoring [11,12]. In early studies, primarily single indices, such as the vegetation index [13], surface temperature [14], and impervious surface cover [15], were used, thereby capturing only specific ecological features. To address this limitation, multiple indicator approaches have been explored [16,17], with the remote sensing ecological index (RSEI) emerging as a prominent method [18]. The RSEI conforms with the stress–state–response model widely employed in ecological research and has been applied to various geographic units, such as watersheds [19,20], mines [21], cities [22], and ecological reserves [23], yielding meaningful results due to its objectivity and comprehensiveness. Importantly, although many scholars have adjusted the indices to better suit regional characteristics [24–26], Xu et al. emphasized that the development and improvement of remote sensing models must be thoroughly justified in terms of the rationality and appropriateness of key algorithms [27–29]. This further validated the positive contribution of the original RSEI to ecological research. Moreover, when long-term and large-scale RSEI analysis is performed, traditional evaluation methods face challenges because of the massive volume of data and complex processing requirements. The Google Earth Engine (GEE) platform overcomes these challenges by providing powerful computational capabilities for efficient data processing [30] and has been widely applied in ecological assessments [31–33].

Although the application of the RSEI has become increasingly widespread, research gaps remain in its application and accuracy enhancement within specific watersheds. Furthermore, while existing studies have explored the RSEI in large geographic regions [12,32,34], particularly the Loess Plateau, there is still insufficient understanding of its long-term spatial–temporal variations and the impacts of both natural and anthropogenic factors. To address this gap, this study focuses on the upper-middle Fen River Basin (UMFRB), which lies at the junction of the northern sand control belt and the Loess Plateau–Sichuan–Yunnan Ecological Barrier within China's "Two Screens and Three Belts" ecological security framework [35]. As a critical ecological barrier to the west of the Beijing–Tianjin–Hebei region and the "Water Tower" of the Sanjin area, the basin plays a vital role in regional ecological security. However, severe soil erosion across the Loess Plateau has rendered the region ecologically fragile. In addition, the high population density and extensive exploitation of coal and mineral resources have further exacerbated the vulnerability of the basin's ecosystem [36]. Therefore, long-term monitoring of the ecological quality in the UMFRB will not only reveal the spatial–temporal patterns of the region but also provide deeper insights into the dual impacts of both natural and anthropogenic factors on ecosystem health.

The main objectives of this study are as follows: (1) to calculate the RSEI for the UMFRB from 2000 to 2023 via the GEE platform and to monitor the long-term ecological quality changes in the region; (2) to analyze the spatial–temporal characteristics, trends, and consistency of the ecological quality over time; and (3) to explore the impacts of natural and anthropogenic factors on the ecological quality variations in the UMFRB. Through this study, we aim to provide systematic insights into the ecological protection and sustainable development of typical Loess Plateau watersheds and to contribute to the improvement of the ecological environment in this region.

2. Study Area and Data Sources

2.1. Study Area

The UMFRB is located in the eastern part of the Loess Plateau of China (111°3′–113°27′ E, 36°40′–39°8′ N). It encompasses the area where the main stream of the Fen River and its tributaries flow from the Leimingsi Spring in Ningwu County to the Wangjiazhuang section in Lingshi County [37] (Figure 1). The basin covers a total area of 27,213.57 km^2

and includes 25 county-level administrative regions as of 2024. The terrain of the study area is rugged, with elevations ranging from 635 to 2824 m. The UMFRB has a continental monsoon climate, with an average annual temperature between 7.0 °C and 13.7 °C and an average annual precipitation of approximately 500 mm. The study area features fragmented and discontinuous natural woodlands and other high-quality ecological spaces [38], and it also faces significant ecological challenges, including water scarcity, severe soil erosion, environmental degradation resulting from mining activities, and loss of biodiversity [39].

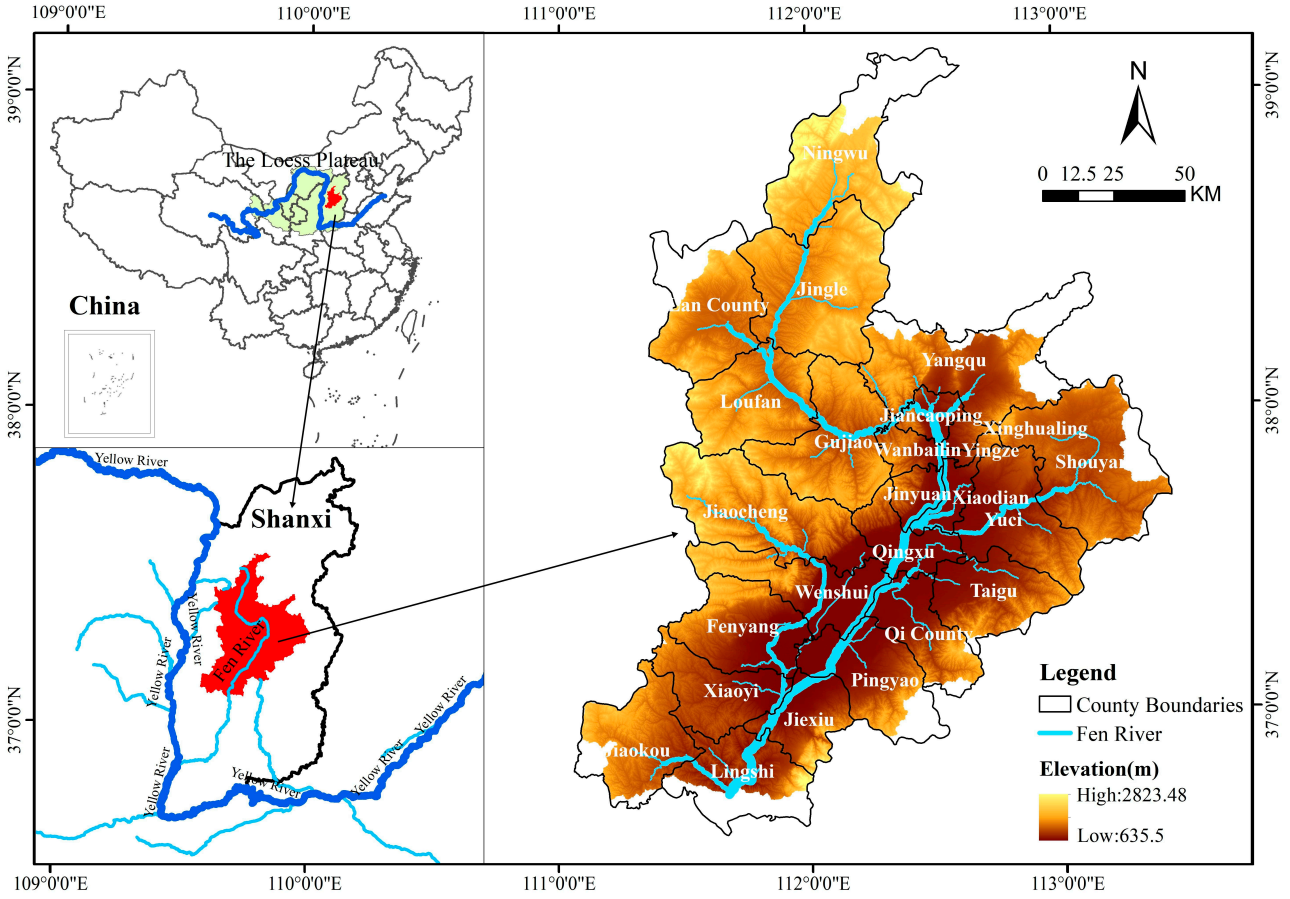


Figure 1. Location of the study area.

2.2. Data and Preprocessing

In this study, remote sensing data were obtained via the GEE platform, accessing radiometrically, atmospherically, and geometrically corrected Landsat 5 TM, Landsat 7 ETM+, and Landsat 8 OLI/TIRS surface reflectance datasets. Specifically, Landsat 5 TM data (ID: "LANDSAT/LT05/C02/T1_L2") were used for the period from 2000 to 2011, Landsat 7 ETM+ data (ID: "LANDSAT/LE07/C02/T1_L2") were used for 2012, and Landsat 8 OLI/TIRS data (ID: "LANDSAT/LC08/C02/T1_L2") were used for 2013–2023. All three datasets have a spatial resolution of 30 m. Remote sensing images covering the study area during the vegetation growing season (June to September) with less than 50% cloud cover were selected [27]. The United States Geological Survey (USGS)-approved Landsat cloud removal algorithm (CFMASK) was then applied to eliminate cloud interference [40], followed by median synthesis to create a clear composite image, which was cropped to ensure alignment with the boundaries of the study area. Water bodies were masked out via the modified normalized difference water index (MNDWI) [41]. Image synthesis was required for surface temperature inversion in the study area because of the limitation of Landsat image width in calculating the land surface temperature (LST). However, this approach can cause time–phase differences near the stitching lines, resulting in notice-

able stripping effects, as shown in Figure 2, which presents a significant challenge for subsequent analysis and evaluation. To overcome this issue, we selected the Moderate Resolution Imaging Spectroradiometer (MODIS) surface temperature product MOD11A2 (ID: MODIS/061/MOD11A2) with a 1 km resolution. Given the spatial autocorrelation of land surface temperature, MOD11A2 remains a reliable choice for capturing stable surface temperature data across large study areas, despite the resolution trade-off [42].

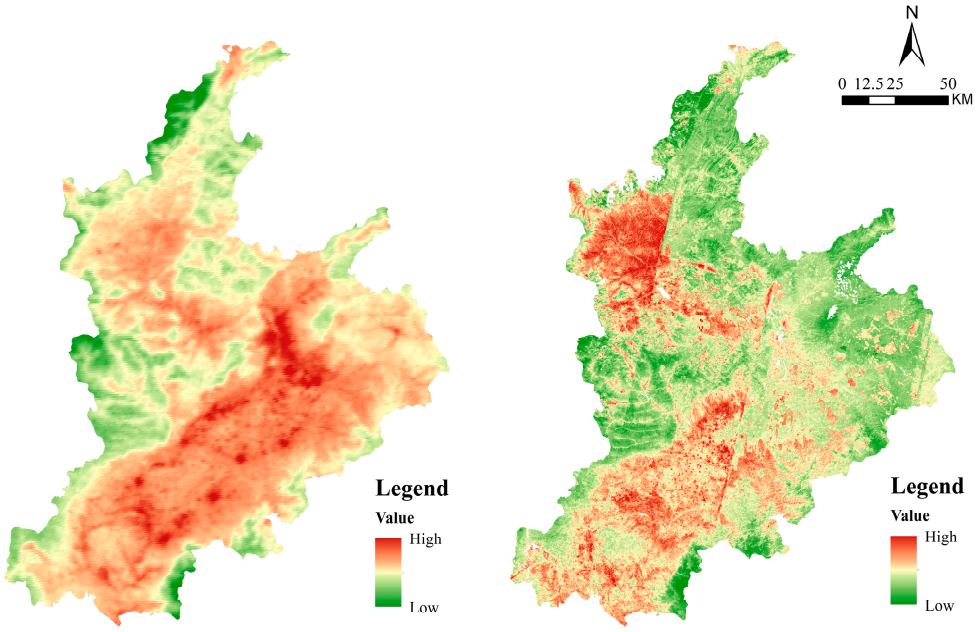


Figure 2. Comparison of LST from MOD11A2 and Landsat Inversion in 2020.

Furthermore, physical geographic and socioeconomic data, including digital elevation model (DEM), slope (SLO), precipitation (PRE), temperature (TEM), gross domestic product (GDP), population density (POP), nighttime light index (NLI), and land use type (LUT) data, were collected, as detailed in Table 1. All the data were reprojected to the WGS_1984_UTM_Zone_49N coordinate system, and the raster data were resampled to a resolution of 30 m × 30 m.

Table 1. Physical geographic and socioeconomic data types and sources.

Data Types	Dataset	Source	Spatial Resolution
DEM	COPERNICUS/DEM/GLO30	GEE (https://earthengine.google.com/ (accessed on 20 June 2024))	30 m
SLO	COPERNICUS/DEM/GLO30		30 m
PRE	Average annual precipitation dataset of China (1901–2022)	Geographic Data Sharing Infrastructure, global resources data cloud (http://www.gis5g.com)	1000 m
TEM	1901–2022 year-by-year mean temperature raster dataset	National Tibetan Plateau/Third Pole Environment Data Center (http://data.tpdc.ac.cn/)	1000 m
GDP	China GDP spatial distribution kilometer grid dataset	Resource and Environmental Science Data Platform (https://www.resdc.cn)	1000 m
POP	China population spatial distribution kilometer grid dataset		1000 m

Table 1. *Cont.*

Data Types	Dataset	Source	Spatial Resolution
NLI	2000–2023 global-scale class National Polar-Orbiting Partnership (NPP)-Visible Infrared Imaging Radiometer Suite (VIIRS) nighttime light data	An extended time-series of global NPPVIIRS-like nighttime light data (https://doi.org/10.7910/DVN/YGIVCD)	500 m
LUT	China multiperiod land use remote sensing monitoring dataset (CNLUCC)	Resource and Environmental Science Data Platform (https://www.resdc.cn)	30 m

3. Methodology

The research methodology in this study comprises three main components (Figure 3). First, the RSEI for the UMFRB was calculated for the 2000–2023 period via the GEE platform. Second, the trends in the RSEI were quantified via Sen's slope estimation and the Mann–Kendall test, and future consistency was determined via the Hurst exponent method. Finally, the spatial autocorrelation of the RSEI was verified via Moran's I, while the driving factors influencing the RSEI in the UMFRB were analyzed via Pearson's correlation analysis and the geographically weighted regression (GWR) model.

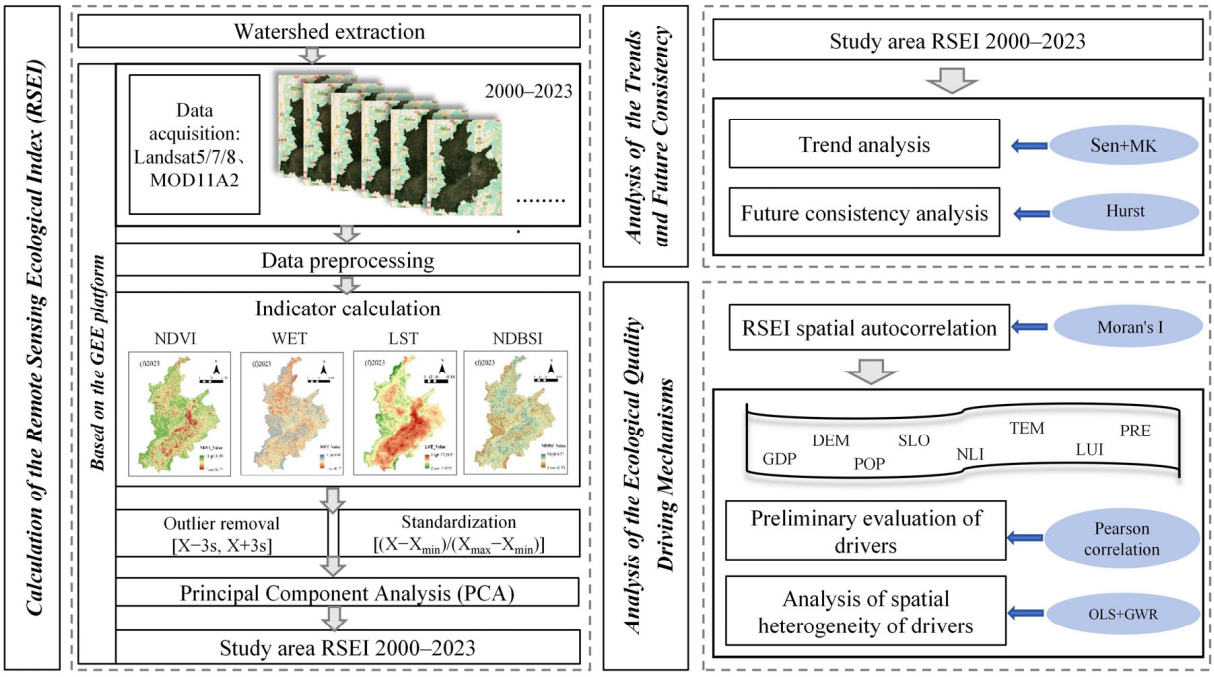


Figure 3. Overview of the methodology.

3.1. Calculation of the RSEI

The RSEI integrates four key ecological factors that are easily perceived by humans: greenness, wetness, heat, and dryness. These indices are derived entirely from readily available remote sensing data, with no manual intervention in the calculation process, thus ensuring the reliability and comparability of the results. Specifically, greenness, wetness, heat, and dryness are represented by the normalized difference vegetation index (NDVI) [43], wetness component (WET) [44,45], land surface temperature (LST) [46], and normalized difference built-up and soil index (NDBSI) [18], respectively. The calculation equations are detailed in Table 2.

Table 2. Calculation equations for the NDVI, WET, LST, and NDBSI.

Index	Equation
NDVI	$NDVI = (\rho_{NIR} - \rho_R)/(\rho_{NIR} + \rho_R)$
WET	$WET = 0.0315\rho_B + 0.2021\rho_G + 0.3012\rho_R + 0.1594\rho_{NIR} - 0.6806\rho_{SWIR1} - 0.6109\rho_{SWIR2}$(Landsat TM, Landsat ETM+) $WET = 0.1511\rho_B + 0.1973\rho_G + 0.3283\rho_R + 0.3407\rho_{NIR} - 0.7117\rho_{SWIR1} - 0.4559\rho_{SWIR2}$(Landsat OLI)
LST	$LST = 0.02 \times LST_Day_1\ km - 273.5$
NDBSI	$NDBSI = (SI + IBI)/2$ $SI = \frac{(\rho_{SWIR1}+\rho_R)-(\rho_{NIR}+\rho_B)}{(\rho_{SWIR1}+\rho_R)+(\rho_{NIR}+\rho_B)}$ $IBI = \frac{\frac{2\rho_{SWIR1}}{\rho_{SWIR1}+\rho_{NIR}} - \left(\frac{\rho_{NIR}}{\rho_{NIR}+\rho_R} + \frac{\rho_G}{\rho_G+\rho_{SWIR1}}\right)}{\frac{2\rho_{SWIR1}}{\rho_{SWIR1}+\rho_{NIR}} + \left(\frac{\rho_{NIR}}{\rho_{NIR}+\rho_R} + \frac{\rho_G}{\rho_G+\rho_{SWIR1}}\right)}$

Notes: ρ_B, ρ_G, ρ_R, ρ_{NIR}, ρ_{SWIR1}, ρ_{SWIR2} represent the Landsat 5 TM, Landsat7 ETM+ and Landsat 8 OLI/TIRS bands, respectively. *SI* represents the soil index, and *IBI* represents the building index.

The four component indicators were combined via principal component analysis (PCA), with the RSEI constructed from the first principal component (PC1). Since the indicators varied in magnitude, the direct application of PCA could lead to imbalanced weights. To address this issue, the four indicators were first normalized to the [0, 1] range before PCA was performed. Additionally, to prevent outliers from skewing the results, the three-standard-deviation method was employed to remove extreme values from the images. The wetness component, which is less affected by seasonal variations, was selected to determine the direction of the eigenvector of PC1 [47], as determined via Equation (1).

$$RSEI_0 = \begin{cases} PC1[f(NDVI, WET, NDBSI, LST)], \lambda_{Wet} \geq 0 \\ 1 - PC1[f(NDVI, WET, NDBSI, LST)], \lambda_{Wet} < 0 \end{cases} \quad (1)$$

where λ_{Wet} is the direction of contribution of the wetness component to the PC1 function.

The RSEI was further normalized to obtain the final value, as expressed in Equation (2).

$$RSEI = (RSEI_0 - RSEI_{0_min})/(RSEI_{0_max} - RSEI_{0_min}) \quad (2)$$

where $RSEI_0$, $RSEI_{0_max}$, and $RSEI_{0_min}$ are the initial, maximum, and minimum values of the RSEI, respectively.

The final RSEI values range from 0 to 1, with values closer to 1 indicating higher ecological quality. On the basis of previous studies [21,22], the RSEI values in this study were categorized into five classes for spatial display: excellent ($0.8 < RSEI \leq 1$), good ($0.6 < RSEI \leq 0.8$), moderate ($0.4 < RSEI \leq 0.6$), fair ($0.2 < RSEI \leq 0.4$), and poor ($0 < RSEI \leq 0.2$).

3.2. Analysis of the Trends and Future Consistency

3.2.1. Sen's Slope Estimation and Mann–Kendall Test Methods

To quantitatively assess the trend in the ecological quality changes in the study area from 2000 to 2023, Sen's slope estimation method was employed to fit the change trajectory of the RSEI on the basis of the image data [48]. Sen's slope estimation method is computationally efficient, is robust against measurement errors, and minimizes the influence of outliers, making it ideal for analyzing long-term trends in time series data. This method can be expressed as follows [48]:

$$\beta = Median\left(\frac{RSEI_j - RSEI_i}{j - i}\right), n > j > i > 0 \quad (3)$$

where β is the trend degree of the series, Median denotes the median, i and j are the i-th and j-th positions of the time series, respectively, and $RSEI_i$ and $RSEI_j$ are the i-th and j-th RSEI pixel values, respectively.

The significance of the trend analysis results must be assessed. The Mann–Kendall test method, a nonparametric statistical method, offers the advantage of not requiring the data to follow a specific distribution, rendering it highly resistant to data errors [49]. This test method performs well alongside Sen's slope estimation method for analyzing and determining trends in long-term series data and has been widely applied in the analysis of spatial and temporal processes such as vegetation, precipitation, and temperature studies [50,51]. The criteria for evaluating trends in the RSEI in this study are detailed in Table 3.

Table 3. Classification of RSEI trends from 2000 to 2023.

β	Z	Trend Categories	Trend Characteristics
$\beta > 0.0005$	$\|Z\| \geq 1.96$	3	Significant increase
	$1.96 > \|Z\| \geq 1.65$	2	Slightly significant increase
	$\|Z\| < 1.65$	1	No significant increase
$-0.0005 \leq \beta \leq 0.0005$	$\|Z\|$	0	Relative stability
$\beta < -0.0005$	$\|Z\| < 1.65$	−1	No significant decline
	$1.96 > \|Z\| \geq 1.65$	−2	Slightly significant decline
	$\|Z\| \geq 1.96$	−3	Significant decline

Notes: when $|Z| \geq 1.96$, the result passes the 95% confidence level test; when $|Z| \geq 1.65$, the result passes the 90% confidence level test.

3.2.2. Hurst Index

The Hurst index can be used for quantitatively describing the long-term dependence of time series and for analyzing the future RSEI consistency [52,53]. The Hurst index is based on the rescaled range (R/S) analysis method, and the values of the Hurst index vary between 0 and 1. H = 0.5 indicates a random sequence; for 0 < H < 0.5, the future trend is the opposite of the past trend, with values close to 0 indicating greater anti-consistency; and for 0.5 < H < 1, the future trend aligns with the past trend, with values close to 1 indicating greater consistency [54].

3.3. Analysis of the Driving Mechanisms of the Ecological Quality

3.3.1. Spatial Correlation

The spatial autocorrelation of the RSEI is a key indicator that indicates whether the ecological quality of a given element is related to that in its neighboring areas [55], serving as a prerequisite for applying the GWR model [56]. Global Moran's I and local Moran's I were used to assess the spatial autocorrelation of the RSEI. The value of the global Moran's I ranges from 0 to 1, with values close to 1 indicating greater overall spatial autocorrelation. Local Moran's I is a type of local indicator of spatial association (LISA) that can effectively reflect the correlation of the local ecological environment quality in the study area. The LISA clustering map shows five types of local spatial aggregation: high–high (H–H), low–low (L–L), low–high (L–H), high–low (H–L), and not significant. H–H indicates high ecological quality in both the study unit and its neighboring areas, whereas L–L indicates low quality in both. L–H indicates a low-quality study unit with high quality in its neighboring areas, and H–L indicates the opposite.

3.3.2. Factor Selection and Pearson's Correlation

On the basis of the literature and considering the availability and representativeness of data [57,58], four natural factors, namely, DEM, SLO, TEM, and PRE, and four socioeconomic indicators, namely, GDP, POP, NLI, and the land use intensity index (LUI), were selected for a total of eight potential driving factors. LUI is a composite reflection of the extent of land use in a given area, with the following Equation (4) [59]:

$$LUI = 100 \times \sum_{i=1}^{n} A_i \times C_i \quad (4)$$

where A_i is the index of land use degree classification of level i and where C_i is the percentage of area of level i land use degree classification.

The effects of these factors on the ecological environmental quality in the UMFRB were explored. Pearson's correlation analysis was conducted between the RSEI and each explanatory variable for each year to preliminarily evaluate the impacts of these factors on the ecological environment.

3.3.3. Geographically Weighted Regression

In driving factor analysis studies, traditional linear regression models such as the ordinary least squares (OLS) model have been employed to estimate parameters only on average or globally. However, in large-scale spatial studies, different regions may exhibit distinct driving mechanisms, which can lead to inaccuracies in the results of OLS models [60]. The GWR model addresses this shortcoming by incorporating the spatial characteristics of sample point data into the regression parameters, allowing the relationships between variables to vary with spatial location. This approach overcomes the issues of spatial non-stationarity and dependence. The GWR model can be expressed as follows:

$$Y_i = \beta_0(u_i, v_i) + \sum_k \beta_k(u_i, v_i)X_{ik} + \varepsilon_i \quad (5)$$

where Y_i is the RSEI value of cell i; (u_i, v_i) denotes the geographic coordinates of the center of the cell; $\beta_k(u_i, v_i)$ is the regression coefficient of cell i; $\beta_0(u_i, v_i)$ is a constant; X is the matrix of explanatory variables; and ε_i is the random error term.

In this study, the RSEI in each year was set as the dependent variable in the GWR model, with the selected driving factors employed as independent variables. The commonly used adaptive quadratic kernel function was chosen, and the corrected Akaike information criterion (AICc) was used for bandwidth selection. Additionally, a global regression analysis was conducted via the OLS model, and the results were compared with those of the GWR model. In addition to adjusted R-squared values, the AICc values of the two models were compared, with a lower AICc value indicating a better fit to the observed data. If the AICc difference between the two models exceeds 3, the model with the lower AICc value is considered to achieve superior performance [61].

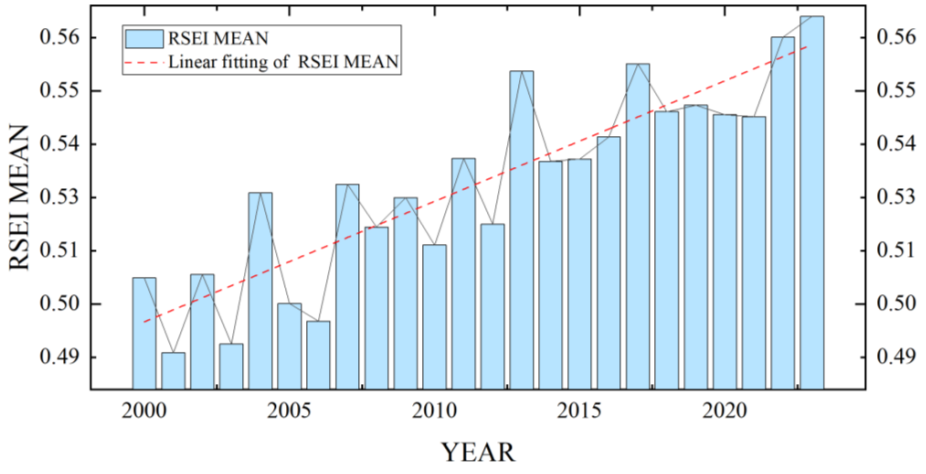
In addition, the RSEI was presented in the form of raster data in space. Therefore, it is essential to create appropriately sized grids and extract values of both the RSEI and its driving factors from these grids before performing spatial autocorrelation and driving factor analysis. However, previous studies have indicated that grid homogeneity increases with increasing analysis scale. If the grid size is very large, valuable information within the grids may be lost, and the spatial autocorrelation of the RSEI could diminish [62]. On the basis of the literature and the scale of the study area, the fishnet tool in ArcMap10.8 was employed to generate grids with sizes of 1, 2, 3, and 5 km [58,63]. Multiple tests revealed that the use of the 3 km grid produced the most accurate and reasonable results for the study area.

4. Results

4.1. Spatiotemporal Characteristics of the Ecological Quality

4.1.1. Temporal Dynamics of the Ecological Quality

The RSEI of the UMFRB showed a fluctuating upward trend from 2000 to 2023. The multiyear average RSEI was 0.53, with an overall increase of 0.06, indicating an increase in the regional ecological quality (Figure 4). The highest average RSEI value was recorded in 2023, at 0.57, whereas the lowest was recorded in 2001, at 0.49. The fluctuations in the RSEI were greater between 2000 and 2005 than they were in the other years. From 2005 to 2010, the RSEI MEAN values were mostly approximately 0.50–0.53, indicating a relatively stable period compared with the early years. From 2010 to 2023, the RSEI MEAN values generally exhibited an increasing trend, with some minor fluctuations. In particular, from 2016 to 2023, the values were consistently high, mostly above 0.54.



RSEI	2000	2001	2002	2003	2004	2005	2006	2007	2008	2009	2010	2011	2012	2013	2014	2015	2016	2017	2018	2019	2020	2021	2022	2023
MEAN	0.51	0.49	0.51	0.49	0.53	0.50	0.50	0.53	0.52	0.52	0.51	0.53	0.52	0.55	0.53	0.53	0.54	0.56	0.55	0.55	0.54	0.54	0.56	0.57
STD	0.16	0.16	0.15	0.16	0.16	0.16	0.17	0.15	0.15	0.16	0.16	0.16	0.15	0.16	0.16	0.16	0.16	0.16	0.15	0.17	0.16	0.16	0.16	0.17

Figure 4. RSEI time series plot, 2000–2023.

4.1.2. Spatial Dynamics of the Ecological Quality

In terms of spatial distribution, the RSEI values in the UMFRB demonstrated significant spatial variability, as shown in Figure 5. From 2000 to 2023, the areas classified as excellent and good steadily expanded, whereas those classified as poor and fair contracted. Specifically, in 2000, areas classified as poor and fair were concentrated in the southern and northern regions. By 2005, the ecological quality in the southern region increased, and areas with poor ecological quality shifted northward, particularly near Taiyuan and the upper reaches of the Fen River. After 2010, the ecological quality in these northern areas, including Taiyuan, increased, leaving areas categorized as poor and fair more sporadically scattered. Overall, better ecological conditions were observed in Pangquangou National Forest Park in Jiaocheng County (west) and Luye Mountain National Nature Reserve at the headwaters of the Fen River (northwest), whereas poorer conditions were concentrated along both sides of the Fen River and in urban areas.

In terms of proportion, the moderate grade consistently accounted for the largest share, whereas the poor grade accounted for the smallest share. Except in 2005, areas classified as poor and fair exhibited a 10% decrease over time, whereas areas classified as excellent and good increased by 18%, indicating significant ecological improvement. The highest proportion of poor and fair grades was recorded in 2005, accounting for 31% of the total amount. In that year, the proportion of poor and fair grades was the only instance where it exceeded the proportion of excellent and good grades, reflecting a mid-range deviation in ecological quality. Furthermore, from 2020 to 2023, the most rapid increase in the proportions of excellent and good ratings occurred, increasing by 6% and 4%, respectively.

4.2. Analysis of RSEI Change Trends and Future Consistency

4.2.1. Spatial and Temporal Trends in the Ecological Quality

The Sen's slope estimation and Mann–Kendall test results indicated that 52.78% of the study area exhibited an increasing trend in the RSEI from 2000 to 2023, while 9.47% showed a declining trend, and 37.75% exhibited no significant trend (Figure 6). Among the areas with an increasing trend, 87.98% demonstrated a significant increase, whereas 81.78% of the declining areas exhibited a significant decline. The areas with declining trends were primarily concentrated in the urban built-up regions of the central plains, surrounded by areas showing no significant trend. This pattern suggests that human activities significantly impact these regions.

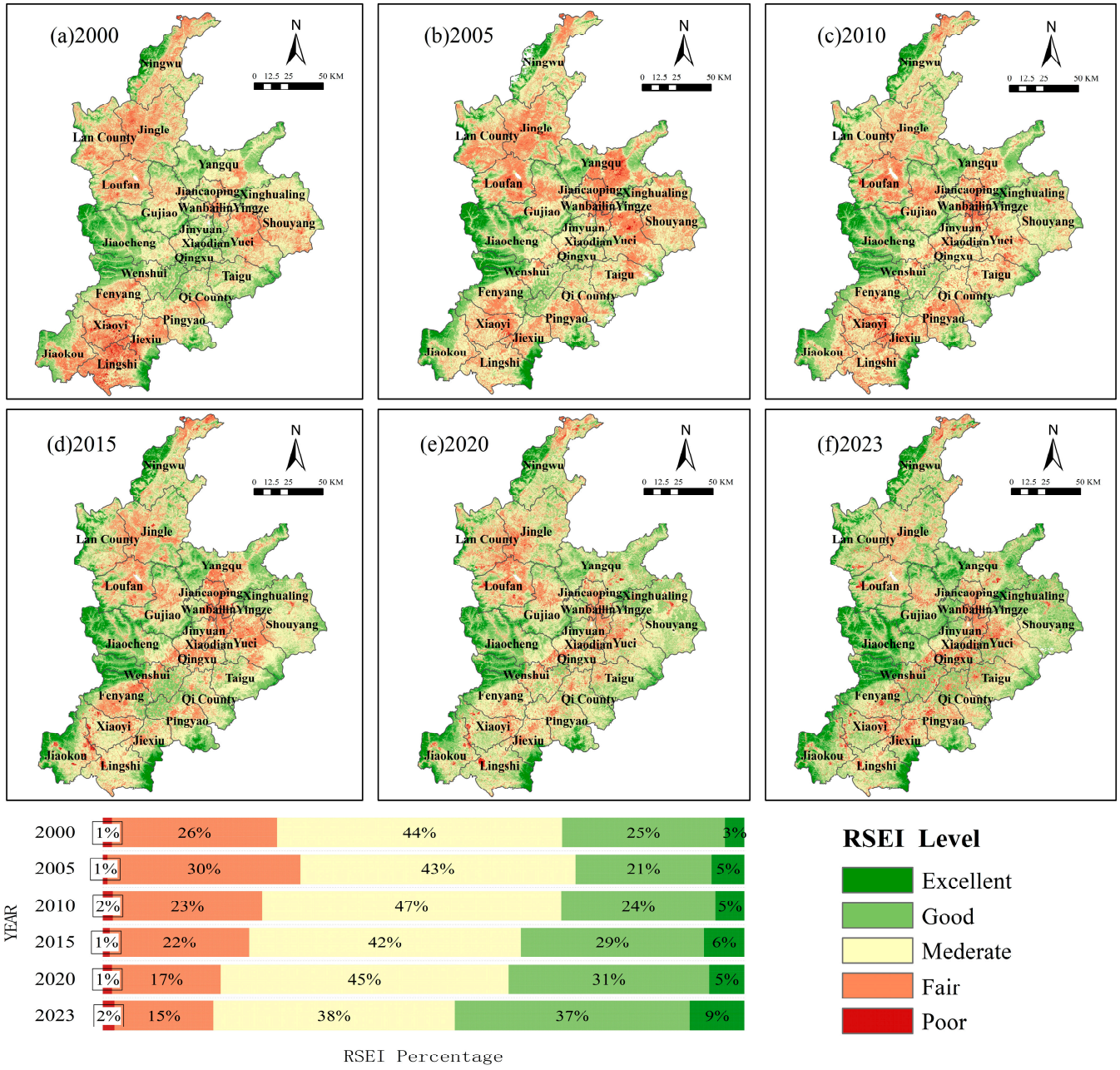


Figure 5. Spatial distributions of the various RSEI classes in the study area. (**a**) RSEI distribution map of 2000; (**b**) RSEI distribution map of 2005; (**c**) RSEI distribution map of 2010; (**d**) RSEI distribution map of 2015; (**e**) RSEI distribution map of 2020; and (**f**) RSEI distribution map of 2023.

4.2.2. Analysis of RSEI Future Consistency

The Hurst index value for the RSEI from 2000 to 2023 was 0.468, indicating anti-consistency and suggesting that the overall ecological environment was in an unstable state (Figure 7a). Areas with Hurst index values less than 0.5 accounted for 63.71% of the study area, indicating that future ecological quality trends are likely to diverge from past patterns. By contrast, 36.29% of the study area presented a Hurst index value greater than 0.5, suggesting that the future ecological environment quality will likely follow the same evolutionary trajectories observed over the past 24 years.

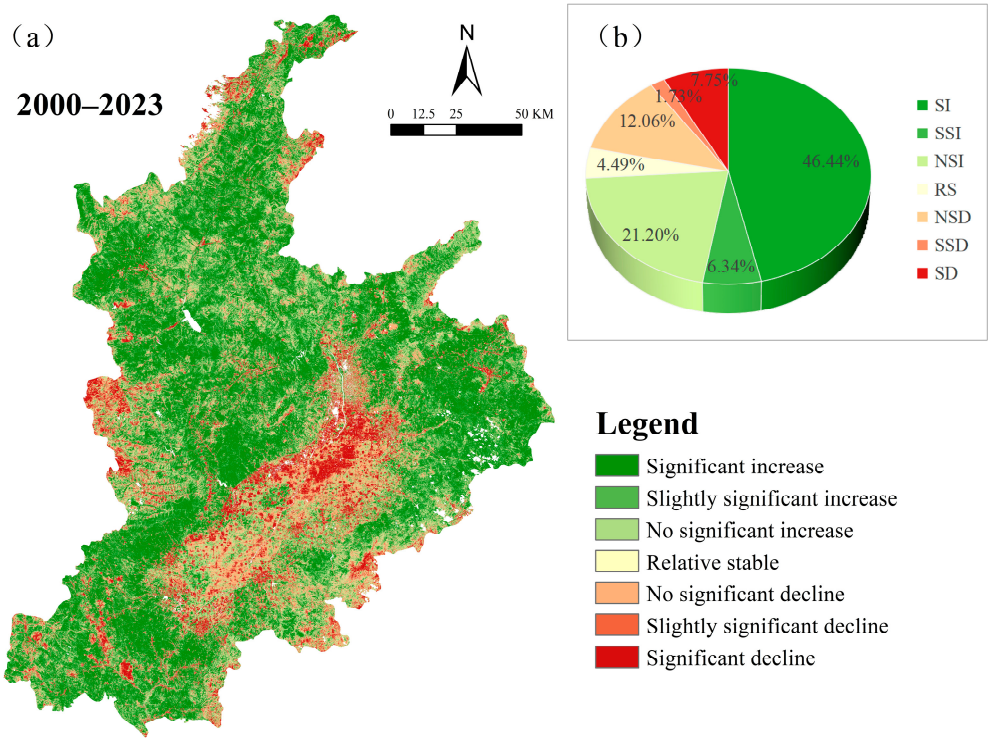


Figure 6. Trends in the RSEI within the study area from 2000 to 2023. (**a**) Spatial distribution of trends and (**b**) proportion of each trend type.

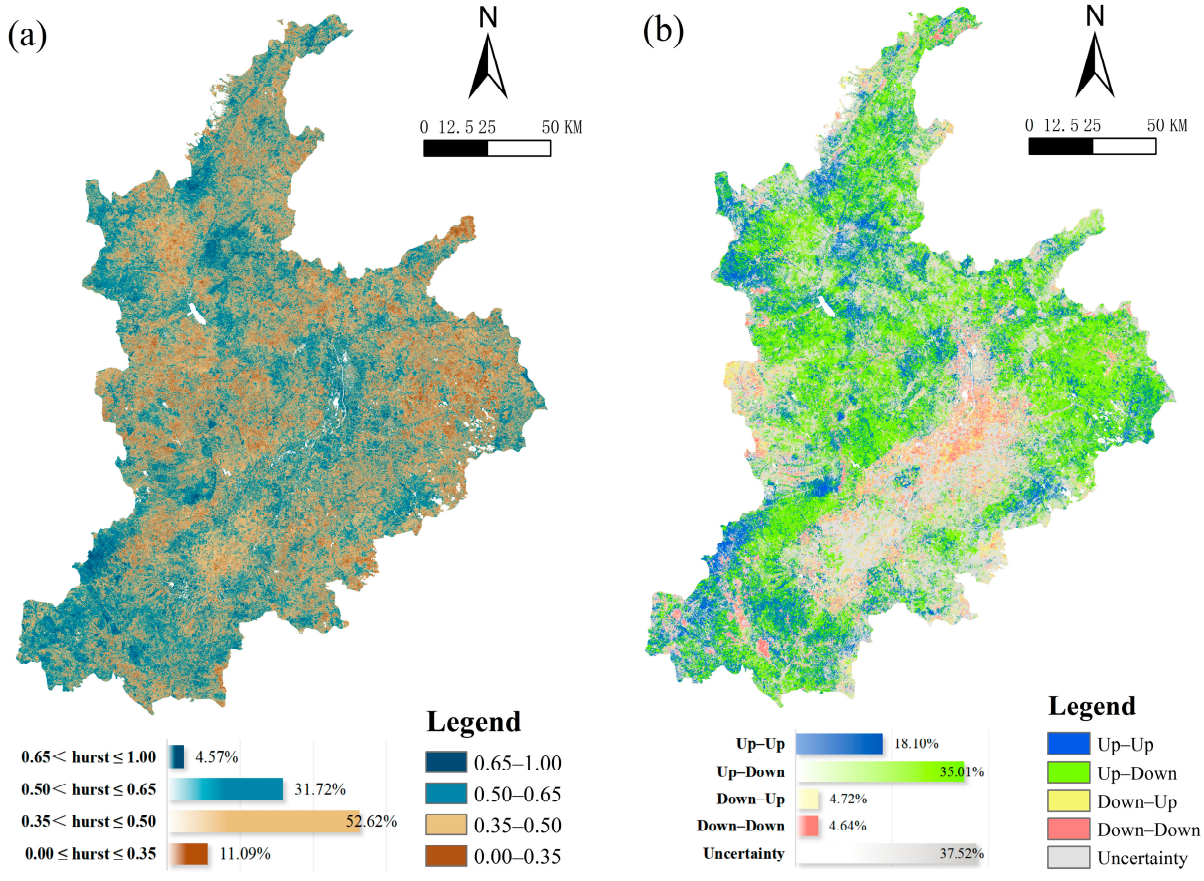


Figure 7. Spatial distributions of the Hurst index values (**a**) and future consistency (**b**).

By integrating the RSEI trend with the Hurst index, we created a consistency pattern map of ecological quality changes in the UMFRB from 2000 to 2023 (Figure 7b). According to this map, the changes can be categorized into five types, namely, continuous degradation (down–down), future degradation (up–down), continuous improvement (up–up), future improvement (down–up), and uncertain change (uncertainty), which account for 4.64%, 35.01%, 18.10%, 4.72%, and 37.52% of the total area, respectively. Continuous degradation (down–down) was primarily found in low-elevation urban built-up areas in the central plains, particularly in Xiaodian District and Qingxu County of Taiyuan city. These areas urgently require improvement while balancing the demands of future economic growth. Areas exhibiting future degradation (up–down) were distributed evenly throughout the study area. To maintain their current good ecological quality, ongoing monitoring will be necessary to prevent further deterioration. The areas demonstrating continuous improvement (up–up) were primarily located in the northwestern and southwestern regions, whereas the areas indicating future improvement (down–up) did not exhibit significant spatial clustering. Uncertain changes were largely concentrated in the central plains, which are densely populated and heavily influenced by anthropogenic factors, showing no clear future development trend.

4.3. Analysis of the Ecological Quality Driving Mechanisms

4.3.1. Spatial Autocorrelation Analysis of the RSEI

Moran's I values of the RSEI in the study area exceeded 0.76 in all years, with Z scores above 75%, thus passing the 1% significance test (Table 4). This indicates a strong positive spatial correlation of the ecological quality in the region, meaning that areas with similar ecological quality levels exhibit significant spatial clustering.

Table 4. Moran's I results.

Year	Global Moran's I	Z Score	*p* Value
2000	0.82	83.28	0.00
2005	0.79	80.68	0.00
2010	0.78	79.15	0.00
2015	0.79	79.97	0.00
2020	0.77	78.27	0.00
2023	0.76	77.26	0.00

The local spatial autocorrelation of the regional RSEI was analyzed via the LISA clustering results. Overall, the nonsignificant areas exhibited a decreasing trend (Figure 8). Area I, located at the junction of Jingle, Lan, and Loufan Counties in the upper Fen River Basin, exhibited a continuous decrease in L–L clusters. Area II, encompassing southern Taiyuan, eastern Wenshui, and western Qixian, exhibited the most significant changes. In 2000, H–H clusters dominated, but after more than 20 years of socioeconomic development, H–H clusters declined, whereas L–L clusters expanded and eventually dominated. Area III, which includes Xiaoyi, Jiexiu, Lingshi, and Jiaokou, initially featured L–L clusters in 2000 and 2010, but the L–L clusters contracted and shifted northward after 2015.

4.3.2. Correlations Between the RSEI and Driving Factors

Values of the RSEI and all its driving factors were extracted into the grid, resulting in 2989, 2920, 2933, 2930, and 2926 samples per image for 2000, 2005, 2010, 2015, and 2020, respectively. Pearson's correlation analysis was conducted to examine the relationships between the RSEI and the corresponding explanatory variables for each year. The results indicated that at a significance level of $\alpha = 0.01$, DEM, SLO, TEM, PRE, POP, NLI, and LUI all passed the significance test each year. However, only GDP in 2000 did not pass the significance test, likely because of a threshold effect, suggesting that the impact of the economy on the ecological environment becomes significant only after reaching a certain development level.

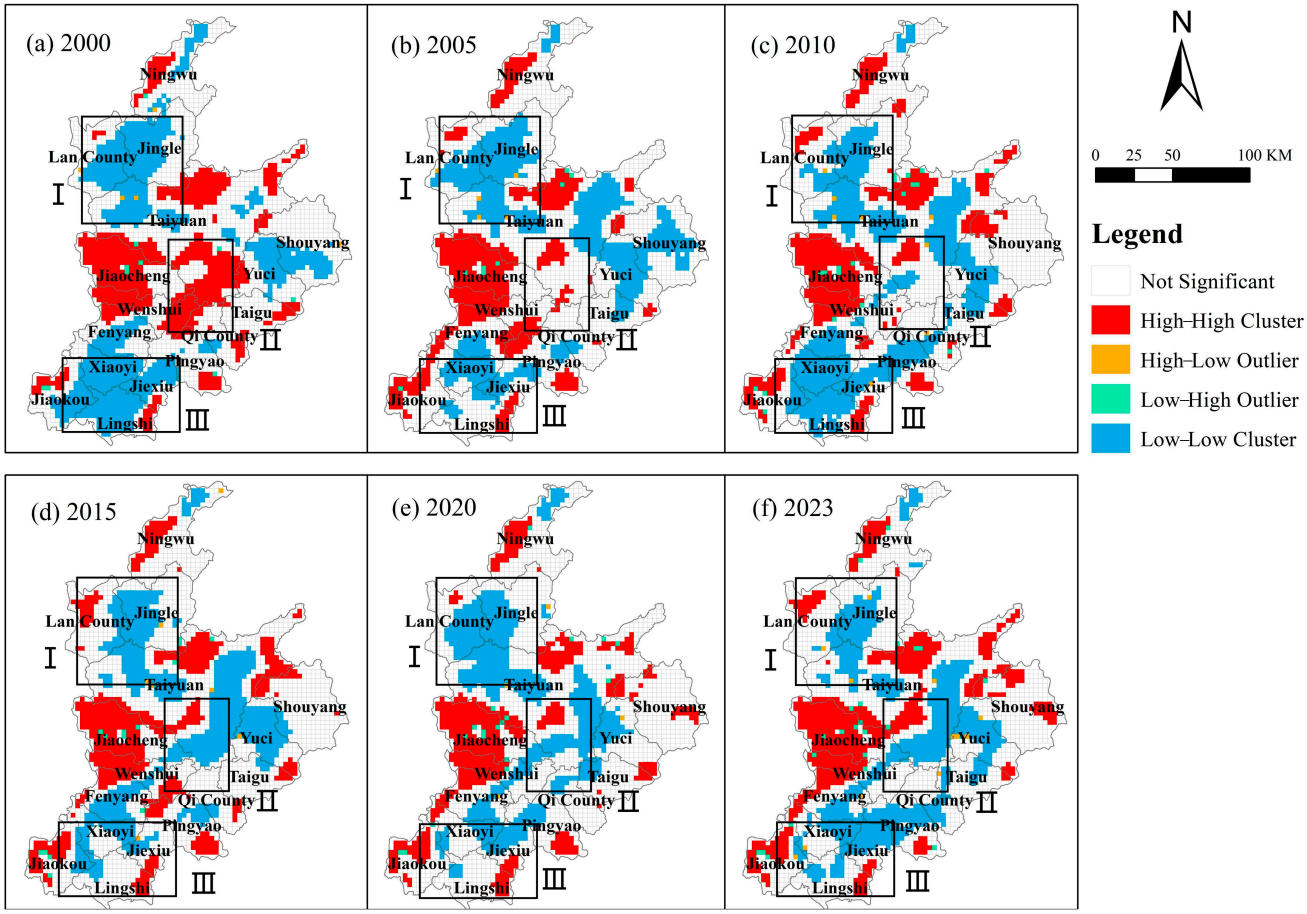


Figure 8. LISA clustering results for the study area.

The multiyear average correlation of each factor with the ecological quality in the UMFRB (Figure 9) decreased in the following order: DEM > TEM > LUI > PRE > SLO > NLI > POP > GDP. DEM and SLO were positively correlated with the RSEI, particularly in 2010 and 2015, suggesting that topographic factors may significantly influence the ecological quality. TEM attained a notable negative correlation with the RSEI, especially in 2015, with a correlation coefficient of −0.595, indicating that increasing temperatures may negatively affect ecological conditions. PRE was positively correlated with the RSEI, particularly in 2010 and 2020, suggesting that increased precipitation increased the ecological quality. Compared with these of the natural factors, human-activity-related factors such as GDP, POP, and NLI exhibited weaker correlations with the RSEI, suggesting that economic development, population density, and nighttime light, respectively, exerted less direct influences during this period. LUI was consistently and strongly negatively correlated with the RSEI, especially from 2010 onward, indicating that relatively high land use intensity significantly caused ecological quality degradation.

4.3.3. GWR-Based Analysis of the Spatial Heterogeneity of Drivers

OLS regression and GWR models were constructed to explore the spatial and temporal differences in the impacts of drivers on the RSEI. For the OLS regression model, the variance inflation factor (VIF) values of SLO and TEM were greater than 7.5, whereas the VIF values of the other influencing factors were less than 7.5, indicating that SLO and TEM were redundant. Therefore, these two variables were removed from the GWR model, and the remaining factors exhibited no multicollinearity.

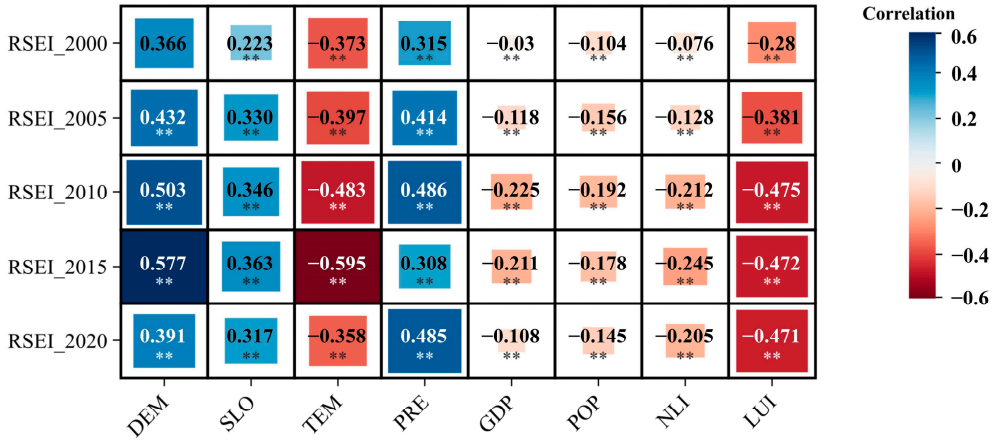


Figure 9. RSEI and driving factor Pearson's correlation (notes: ** indicates significance of the parameters at the 1% level).

The fitting statistics for both the OLS and GWR models are provided in Table 5. The results revealed that the R^2 adjusted value for the goodness-of-fit of the GWR model was significantly greater than that of the OLS model across all years. Additionally, the corrected AICc value for the GWR model was notably lower than that of the OLS model (by more than 3), indicating that the GWR model could better explain the local variations in the RSEI and demonstrated a high degree of reliability.

Table 5. Estimated parameters of the OLS and GWR models.

Year	Ordinary Least Squares (OLS)			Geographically Weighted Regression (GWR)		
	AICc	R^2	Adjusted R^2	AICc	R^2	Adjusted R^2
2000	−3149.021	0.269	0.267	−4749.567	0.541	0.521
2005	−3331.423	0.267	0.265	−5055.437	0.621	0.601
2010	−3541.178	0.287	0.285	−4838.077	0.569	0.549
2015	−3305.794	0.301	0.299	−4122.794	0.482	0.473
2020	−3815.004	0.347	0.345	−4272.088	0.472	0.449

The spatial distribution of the regression coefficients for the remaining independent variables (Figure 10) indicated localized spatial differences in the effects of various drivers on the ecological quality. Specifically, SLO yielded a negative influence in the central plain areas but a significant positive influence in the higher-elevation regions of Ningwu, Jingle, Jiaocheng, and Lingshi Counties. PRE generated a positive influence in most of the study area, although its effect on the RSEI exhibited spatial fragmentation from 2000 to 2020. GDP showed varying influences across cities; it exhibited a negative effect in urban agglomerations in 2010 and 2015 but exhibited a positive effect in the upper Fen River Basin by 2020. POP had a negative influence in the central Taiyuan Basin but a positive influence in the northern headwaters and southern middle reaches of the Fen River. NLI displayed negative influences in the central and southern plains, with a shift from positive to negative influences in the northern region. LUI largely demonstrated negative influences across the study area, although it exhibited a positive trend in parts of the Taiyuan Basin from 2000 to 2010 before becoming negative as land use intensified. Notably, the impacts of GDP, POP, and NLI on the ecological quality in the upper Fen River Basin shifted markedly in 2020, differing significantly from that in previous years.

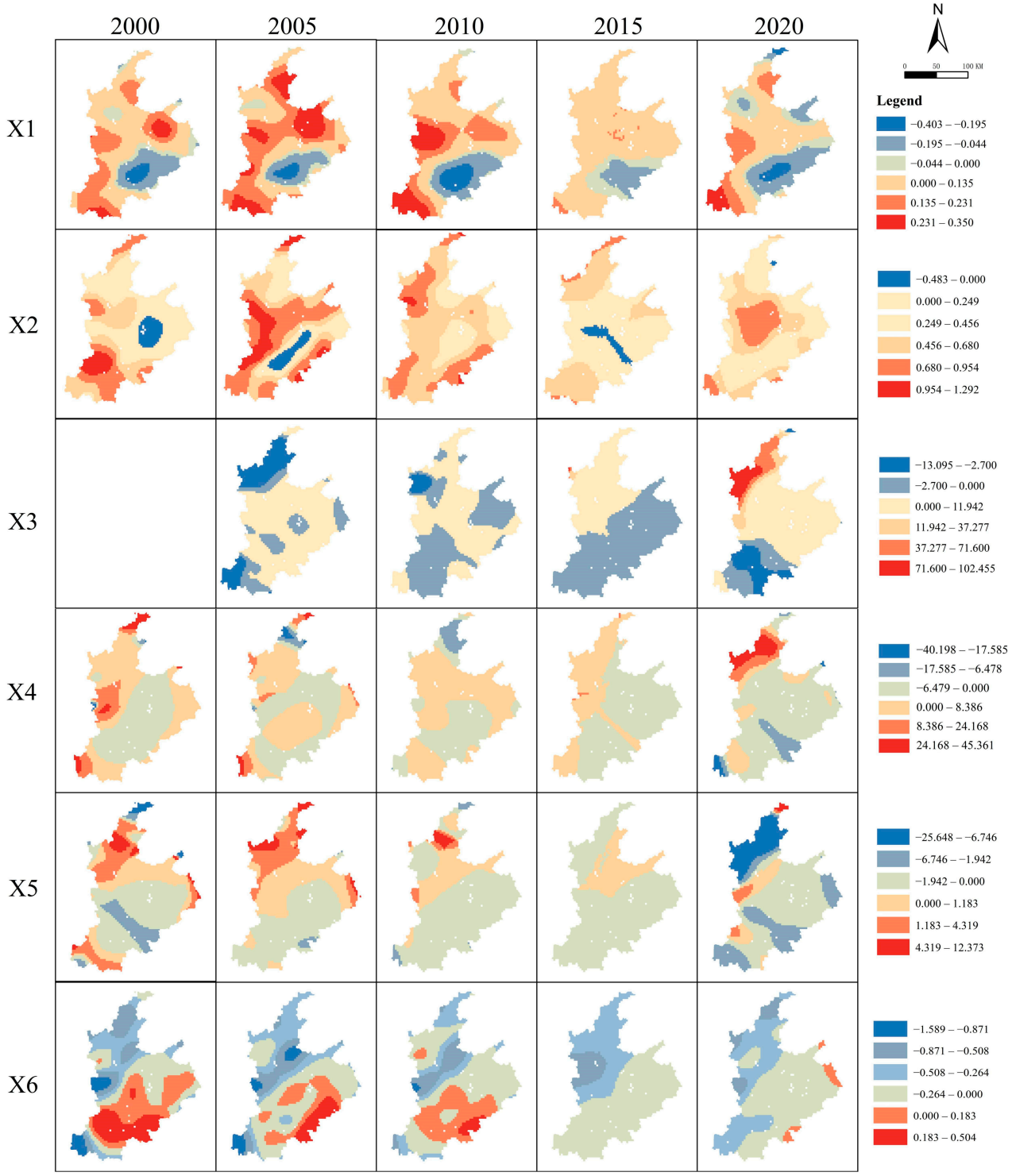


Figure 10. Spatial distribution of the regression coefficients of the GWR model (notes: X1, X2, X3, X4, X5, and X6 denote SLO, PRE, GDP, POP, NLI, and LUI, respectively).

5. Discussion

5.1. Significance of the RSEI for Assessing the Ecological Quality in the Study Area

In this study, the RSEI was employed to assess the quality of the ecological environment in the study area, leveraging its ability to integrate multiple ecological elements. Specifically, the RSEI incorporates key ecological indicators such as the NDVI, WET, LST, and NDBSI to characterize ecosystems from various perspectives. The RSEI values for each year in this study ranged from 0.49 to 0.57, which aligns closely with findings from

related research [58,64], thereby demonstrating the effectiveness of the RSEI in evaluating the ecological quality.

Additionally, the RSEI offers a comprehensive view of the temporal evolution and spatial patterns of the quality of the ecological environment in the study area. With respect to temporal trends, the dynamic changes in the RSEI accurately reflected fluctuations in the ecological quality from 2000 to 2023. From 2000 to 2005, in Shanxi Province, where coal mining is the pillar industry, there was insufficient motivation and capacity to balance economic growth with ecological protection. In combination with climate change impacts [65], this led to substantial fluctuations in the ecological quality during this period. After 2006, Shanxi Province initiated industrial transformation and upgrading [66], optimized ecological restoration policies, and implemented the return of farmland to forests and ecological restoration projects within the basin [67]. Consequently, the quality of the ecological environment in the study area has shown a fluctuating upward trend.

From a spatial perspective, the RSEI effectively highlights regional ecological differences, accurately identifying areas with high or low environmental quality. For example, Pangquangu National Forest Park in the west and Luye Mountain National Nature Reserve at the source of Fen River exhibited relatively high RSEI values, indicating an excellent ecological quality. This suggests that designating key ecologically sensitive areas and reserves within the basin, which represents an important ecological protection initiative, provides essential safeguards for water conservation, soil erosion prevention, and the maintenance of forest landscapes in these fragile ecosystems [68]. Conversely, the banks of the Fen River and urban areas demonstrated lower RSEI values, indicating a lower ecological quality, which is consistent with the findings of related studies [69]. These regions serve as major populations and economic hubs in Shanxi Province and house several coal mining bases, including the Xuangang, Dongshan, Xishan, and Fenxi mining areas [70]. Industrialization has exacerbated soil erosion and environmental pollution due to resource overexploitation, industrial waste discharge, and urban construction encroachment onto land resources, while the dynamics of endogenous economic development remain insufficient [71]. This effective spatial differentiation of the ecosystem quality demonstrates that the RSEI can reasonably reflect the regional ecosystem heterogeneity.

5.2. Analysis of Future Trends and Multifactor Drivers in the Study Area

According to future consistency analysis, 63.71% of the UMFRB is projected to exhibit an anti-consistency trend in the future, with continuous degradation (down–down), future degradation (up–down), and uncertainty accounting for 4.64%, 35.01%, and 37.52% of the total area, respectively. This indicates that the overall ecological environment in the study area is unstable, with low long-term sustainability and dependency on ecological quality trends. Localized ecological restoration has significantly improved environmental quality over the past 24 years, contributing to the overall increase in RSEI levels. However, large areas of the study region are still undergoing degradation or experiencing minimal change, which has led to a general tendency toward reverse persistence in the Hurst index. Furthermore, biodiversity in restored landscapes is often lower than in undisturbed reference landscapes [72]. This is partly due to the use of restoration methods that prioritize fast-growing, highly surviving species, which can exacerbate habitat fragmentation, particularly in ecologically vulnerable and impoverished areas [73]. Additionally, long-term trends may be influenced by cumulative factors such as climate change, urbanization, and land use changes [74], which may not be fully captured in short-term data. Therefore, continuous monitoring and tracking are essential, and efforts to protect the ecological environment remain a long-term challenge [75].

The ecological quality in the UMFRB is influenced by multiple factors. Correlation analysis revealed four natural factors, namely, DEM, TEM, PRE, and SLO, along with socioeconomic factors, such as LUI, as the primary drivers of the ecological quality in the study area. The GWR model further emphasized the varying roles of these factors across the region. In areas with lush vegetation, the RSEI is high and more significantly

influenced by natural factors, whereas socioeconomic factors yield a greater influence in populated plains.

Specifically, among the natural factors, DEM and SLO were positively correlated with the RSEI. Human activities in high-elevation and steep-slope areas are limited by natural conditions, resulting in lower human disturbance and better ecological outcomes. Conversely, SLO in the central plains negatively impacted the RSEI, likely because of the increased convenience for construction and development activities, which can harm the ecological environment [76]. PRE, as a vital water source for vegetation, was positively correlated with the RSEI, especially on the Loess Plateau, where water scarcity directly affects vegetation growth and ecosystem health [58]. The impact of precipitation on the ecosystem exhibits spatial heterogeneity, suggesting that varying degrees of dependence on water resources across the different regions. By contrast, TEM showed a significant negative correlation, particularly within the context of recent warming, as increased temperatures may lead to ecological issues such as drought and water scarcity, adversely affecting the ecological quality.

With respect to human activities, LUI was clearly negatively correlated with the RSEI, especially in areas experiencing rapid urbanization and industrialization. Additionally, NLI reflects the intensity of human activities, with a negative correlation with the RSEI, highlighting the potential harm to the ecological environment stemming from economic development and industrialization. The impacts of GDP and POP on the ecological environment varied across years and regions. Early economic development, characterized by mining and industrial activities, negatively affected the ecological quality. In 2020, the influences of GDP, POP, and NLI on the ecological quality in the upper Fen River Basin changed significantly, which was likely linked to integrated ecological protection and restoration efforts implemented by the Chinese government in the area [77].

5.3. Policy Recommendations and Practical Implications

Owing to the region's historical industrial structure, the basin has long been dependent on resource-based industries such as coal. It is essential to continue advancing industrial transformation, particularly shifting from resource-intensive industries to green, sustainable sectors. This includes promoting the development of low-carbon industries and ecotourism [78]. Furthermore, as a typical hilly region of the Loess Plateau, the study area faces severe soil erosion, water scarcity, and unfavorable terrain and soil conditions for vegetation restoration [79]. It is crucial to implement ecological restoration projects, with more attention given to biodiversity conservation, the greater implementation of nature-based solutions, selecting species that enhance ecological complexity and resilience, and improving ecological connectivity to reduce habitat fragmentation [72]. Third, the urbanization process should integrate ecological considerations into urban planning to ensure policy consistency and long-term effectiveness, which would help reduce the imbalance and recurrence in ecological improvements [80]. Additionally, in the face of challenges posed by climate change, it is important to strengthen climate adaptation measures, promote water-saving technologies, and encourage drought-resistant agricultural practices. Finally, investments in environmental monitoring and data integration should be increased, combining remote sensing data with ground-based observations to support the evaluation of ecological restoration outcomes and long-term monitoring of environmental changes. These measures will contribute to improving ecological quality and achieving sustainable regional development.

5.4. Limitations and Prospects

The long time series of the RSEI and its influencing factors in this study provide valuable insights into the ecological conditions of this region, guiding efforts to enhance regional ecosystem quality and management. However, there are potential limitations and uncertainties. First, this study relied entirely on remote sensing data, which can be constrained by the resolution and quality of the images, potentially introducing errors

in RSEI construction. Second, while the GWR model employed can reveal spatial and temporal differences in the impacts of various drivers on the ecosystem quality, limitations in data access and inconsistencies in the resolution of driver data may affect its explanatory power for the ecosystem quality in the study area.

Ultimately, watersheds are vital for human settlement, and increasing their ecological quality aims to enhance human well-being, which encompasses ecological health, economic development, and overall quality of life. Future research should involve the adoption of comprehensive analytical methods from multiple perspectives to construct a quantitative model linking ecological quality and human well-being in watersheds. This approach can inform the formulation of development strategies that promote the harmonious coexistence of ecology and socioeconomics, thus supporting sustainable development. This direction exhibits both significant opportunities and challenges, potentially offering new ideas and methods for integrated watershed management and long-term development.

6. Conclusions

On the basis of the GEE platform, Landsat image data from 2000 to 2023 were used to construct an RSEI model. A long-term remote sensing evaluation of the quality of the ecological environment in the UMFRB was conducted, and its spatial and temporal characteristics, trends, and consistency were analyzed while exploring the impacts of natural and anthropogenic factors. The study results indicated that the ecological quality in the UMFRB has generally improved over the past 24 years, although certain areas, such as the urban agglomeration of the Taiyuan Basin, have exhibited degradation. The annual mean RSEI value increased from 0.51 to 0.57, with a low ecological quality primarily found along the banks of the Fen River and in urbanized regions. Future consistency analysis revealed that the areas experiencing continuous degradation (down–down), future degradation (up–down), and uncertainty jointly accounted for 77.17% of the study area, highlighting the need for ongoing monitoring and optimized management. In recent years, the ecological quality has demonstrated high spatial aggregation, with positive correlations with DEM, SLO, and PRE and negative correlations with TEM, GDP, POP, NLI, and LUI. The correlations of DEM, TEM, PRE, SLO, and LUI with the ecological quality were notably strong. The effects of various natural and social factors on the RSEI exhibited spatial heterogeneity; areas with lush vegetation, which are more greatly influenced by natural factors, exhibited higher ecological quality, whereas socioeconomic factors significantly impacted the ecological quality in populated plains. This study allows us to better understand the changes and challenges in maintaining the quality of the ecological environment in a timely manner. This understanding is crucial for developing targeted ecological protection and management measures, ultimately enhancing the efficiency of ecological environment management.

Author Contributions: Conceptualization, Y.H. and W.Z.; methodology, Y.H. and B.Y.; software, Y.H. and B.Y.; validation, Y.H. and H.W.; formal analysis, Y.H.; investigation, Y.H. and B.Y.; data curation, Y.H.; writing—original draft, Y.H.; writing—review and editing, Y.H., W.Z. and J.H.; visualization, Y.H. and H.W.; supervision, W.Z.; funding acquisition, J.H. All authors have read and agreed to the published version of the manuscript.

Funding: This research was funded by the National Natural Science Foundation of China (Grant No. 42407626) and the Postdoctoral Fellowship Program of CPSF (Grant No. GZC20241603).

Data Availability Statement: Data will be made available on request.

Acknowledgments: The authors would like to extend their appreciation to all the anonymous reviewers and editors for their constructive comments that improved this paper.

Conflicts of Interest: The authors declare that they have no known competing financial interests or personal relationships that could have appeared to influence the work reported in this study.

References

1. Qiu, J.; Turner, M.G. Spatial interactions among ecosystem services in an urbanizing agricultural watershed. *Proc. Natl. Acad. Sci. USA* **2013**, *110*, 12149–12154. [CrossRef] [PubMed]
2. Feng, J.; Qin, T.; Yan, D.; Lv, X.; Yan, D.; Zhang, X.; Li, W. The role of large reservoirs in drought and flood disaster risk mitigation: A case of the Yellow River Basin. *Sci. Total Environ.* **2024**, *949*, 175255. [CrossRef] [PubMed]
3. Kang, H.; Fu, M.; Kang, H.; Li, L.; Dong, X.; Li, S. The Impacts of Urban Population Growth and Shrinkage on the Urban Land Use Efficiency: A Case Study of the Northeastern Region of China. *Land* **2024**, *13*, 1532. [CrossRef]
4. Plessis, A. du Persistent degradation: Global water quality challenges and required actions. *One Earth* **2022**, *5*, 129–131. [CrossRef]
5. Li, K.; Yang, J.; Wang, J.; Wang, Z.; Zeng, Y.; Borrelli, P.; Hubacek, K.; Hu, Y.; Xu, B.; Fang, N.; et al. Human-altered soil loss dominates nearly half of water erosion in China but surges in agriculture-intensive areas. *One Earth* **2024**, *7*, 2008–2018. [CrossRef]
6. Deng, L.; Guo, Y.; Qi, Y.; Shen, Y.-J.; Shen, Y. Impacts of Climate Change and Human Activities on Streamflow of Upper Yongding River Basin, North China. *Water* **2022**, *14*, 2798. [CrossRef]
7. Xing, X.; Wang, P.; Wang, X.; Yuan, Q.; Hu, B.; Liu, S. Dams alter the control pattern of watershed land use to riverine nutrient distribution: Comparison of three major rivers under different hydropower development levels in Southwestern China. *Water Res.* **2024**, *260*, 121951. [CrossRef]
8. Yan, H.; Lin, Y.; Chen, Q.; Zhang, J.; He, S.; Feng, T.; Wang, Z.; Chen, C.; Ding, J. A Review of the Eco-Environmental Impacts of the South-to-North Water Diversion: Implications for Interbasin Water Transfers. *Engineering* **2023**, *30*, 161–169. [CrossRef]
9. Cui, W.; Liu, J.; Jia, J.; Wang, P. Terrestrial ecological restoration in China: Identifying advances and gaps. *Environ. Sci. Eur.* **2021**, *33*, 123. [CrossRef]
10. Ma, Y.; Wu, H.; Wang, L.; Huang, B.; Ranjan, R.; Zomaya, A.; Jie, W. Remote sensing big data computing: Challenges and opportunities. *Future Gener. Comput. Syst.* **2015**, *51*, 47–60. [CrossRef]
11. Yang, Y.; Erskine, P.D.; Lechner, A.M.; Mulligan, D.; Zhang, S.; Wang, Z. Detecting the dynamics of vegetation disturbance and recovery in surface mining area via Landsat imagery and LandTrendr algorithm. *J. Clean. Prod.* **2018**, *178*, 353–362. [CrossRef]
12. Xu, Y.; Yang, X.; Xing, X.; Wei, L. Coupling eco-environmental quality and ecosystem services to delineate priority ecological reserves—A case study in the Yellow River Basin. *J. Environ. Manag.* **2024**, *365*, 121645. [CrossRef] [PubMed]
13. Gupta, K.; Kumar, P.; Pathan, S.K.; Sharma, K.P. Urban Neighborhood Green Index—A measure of green spaces in urban areas. *Landsc. Urban Plan.* **2012**, *105*, 325–335. [CrossRef]
14. Coutts, A.M.; Harris, R.J.; Phan, T.; Livesley, S.J.; Williams, N.S.G.; Tapper, N.J. Thermal infrared remote sensing of urban heat: Hotspots, vegetation, and an assessment of techniques for use in urban planning. *Remote Sens. Environ.* **2016**, *186*, 637–651. [CrossRef]
15. Hou, Y.; Ding, W.; Liu, C.; Li, K.; Cui, H.; Liu, B.; Chen, W. Influences of impervious surfaces on ecological risks and controlling strategies in rapidly urbanizing regions. *Sci. Total Environ.* **2022**, *825*, 153823. [CrossRef]
16. Tang, D.; Liu, X.; Zou, X. An improved method for integrated ecosystem health assessments based on the structure and function of coastal ecosystems: A case study of the Jiangsu coastal area, China. *Ecol. Indic.* **2018**, *84*, 82–95. [CrossRef]
17. Huang, B.; Li, R.; Ding, Z.; O'Connor, P.; Kong, L.; Xiao, Y.; Xu, W.; Guo, Y.; Yang, Y.; Li, R.; et al. A new remote-sensing-based indicator for integrating quantity and quality attributes to assess the dynamics of ecosystem assets. *Glob. Ecol. Conserv.* **2020**, *22*, e00999. [CrossRef]
18. Xu, H.Q. A remote sensing urban ecological index and its application. *Acta Ecol. Sin.* **2013**, *33*, 7853–7862. [CrossRef]
19. Xiong, Y.; Xu, W.; Lu, N.; Huang, S.; Wu, C.; Wang, L.; Dai, F.; Kou, W. Assessment of spatial–temporal changes of ecological environment quality based on RSEI and GEE: A case study in Erhai Lake Basin, Yunnan province, China. *Ecol. Indic.* **2021**, *125*, 107518. [CrossRef]
20. Yuan, B.; Fu, L.; Zou, Y.; Zhang, S.; Chen, X.; Li, F.; Deng, Z.; Xie, Y. Spatiotemporal change detection of ecological quality and the associated affecting factors in Dongting Lake Basin, based on RSEI. *J. Clean. Prod.* **2021**, *302*, 126995. [CrossRef]
21. Xiao, W.; Guo, J.; He, T.; Lei, K.; Deng, X. Assessing the ecological impacts of opencast coal mining in Qinghai-Tibet Plateau-a case study in Muli coal field, China. *Ecol. Indic.* **2023**, *153*, 110454. [CrossRef]
22. Xu, H.; Wang, Y.; Guan, H.; Shi, T.; Hu, X. Detecting Ecological Changes with a Remote Sensing Based Ecological Index (RSEI) Produced Time Series and Change Vector Analysis. *Remote Sens.* **2019**, *11*, 2345. [CrossRef]
23. Yang, H.; Xu, H. Assessing fractional vegetation cover changes and ecological quality of the Wuyi Mountain National Nature Reserve based on remote sensing spatial information. *J. Appl. Ecol.* **2020**, *31*, 533–542. [CrossRef]
24. Liu, Y.; Dang, C.; Yue, H.; Lyu, C.; Qian, J.; Zhu, R. Comparison between modified remote sensing ecological index and RSEI. *Natl. Remote Sens. Bull.* **2022**, *26*, 683–697. [CrossRef]
25. Zheng, Z.; Wu, Z.; Chen, Y.; Guo, C.; Marinello, F. Instability of remote sensing based ecological index (RSEI) and its improvement for time series analysis. *Sci. Total Environ.* **2022**, *814*, 152595. [CrossRef]
26. Song, M.J.; Luo, Y.Y.; Duan, L.M. Evaluation of ecological environment in the Xilin Gol steppe based on modified remote sensing ecological index model. *Arid Zone Res.* **2019**, *36*, 1521–1527.
27. Xu, H.; Li, M.; Lin, M. Should RSEI Use PCA or kPCA? *Geomater. Inf. Sci. Wuhan Univ.* **2023**, *48*, 506–513. [CrossRef]
28. Xu, H.; Li, C.; Shi, T. Is the z-score standardized RSEI suitable for time-series ecological change detection? Comment on Zheng et al. (2022). *Sci. Total Environ.* **2022**, *853*, 158582. [CrossRef]
29. Xu, H.; Deng, W. Rationality analysis of MRSEI and its difference with RSEI. *Remote Sens. Technol. Appl.* **2022**, *37*, 1–7. [CrossRef]

30. Huang, H.; Chen, W.; Zhang, Y.; Qiao, L.; Du, Y. Analysis of ecological quality in Lhasa Metropolitan Area during 1990–2017 based on remote sensing and Google Earth Engine platform. *J. Geogr. Sci.* **2021**, *31*, 265–280. [CrossRef]
31. Xu, C.; Li, B.; Kong, F.; He, T. Spatial-temporal variation, driving mechanism and management zoning of ecological resilience based on RSEI in a coastal metropolitan area. *Ecol. Indic.* **2024**, *158*, 111447. [CrossRef]
32. Li, Y.; Tian, H.; Zhang, J.; Lu, S.; Xie, Z.; Shen, W.; Zheng, Z.; Li, M.; Rong, P.; Qin, Y. Detection of spatiotemporal changes in ecological quality in the Chinese mainland: Trends and attributes. *Sci. Total Environ.* **2023**, *884*, 163791. [CrossRef] [PubMed]
33. Liao, W.; Jiang, W. Evaluation of the Spatiotemporal Variations in the Eco-environmental Quality in China Based on the Remote Sensing Ecological Index. *Remote Sens.* **2020**, *12*, 2462. [CrossRef]
34. Zhang, L.; Li, X.; Liu, X.; Lian, Z.; Zhang, G.; Liu, Z.; An, S.; Ren, Y.; Li, Y.; Liu, S. Dynamic monitoring and drivers of ecological environmental quality in the Three-North region, China: Insights based on remote sensing ecological index. *Ecol. Inform.* **2025**, *85*, 102936. [CrossRef]
35. Fu, Y.; Shi, X. Ecological restoration zoning of county-level territorial space based on small watershed scale: A case study of the upper Fenhe River in Shanxi. *J. Nat. Resour.* **2023**, *38*, 1225–1239. [CrossRef]
36. Yuan, D.; Dong, J. Research on ecological restoration and its impact on society in coal resource-based areas: Lessons from the Ruhr area in Germany and the Liulin area in China. *Geoforum* **2024**, *154*, 104038. [CrossRef]
37. Regulations on Water Resource Management and Water Environment Protection in the Upper and Middle Fen River Basin of Shanxi Province. Available online: http://asianlii.austlii.edu.au/chi/cn/legis/sx/laws/8c80e17b0b7e8d8fa9a7ccc2c846a798cec4ef20/ (accessed on 25 October 2024).
38. Wang, Y.; Bai, Q.; Sun, H. Spatial-temporal evolution and driving factors of ecological vulnerability in Fenhe River Basin from 2000–2020. *J. Zhejiang Univ. Sci. Ed.* **2023**, *50*, 607–618. [CrossRef]
39. Zhou, W.; Guan, Y.J.; Liu, Q.; Fan, Y.B.; Bai, Z.K.; Shi, X.Y.; Hu, Y.C.; Huang, Y.H.; Bai, D.S. Diagnosis of ecological problems and exploration of ecosystem restoration practices in the typical watershed of loess plateau: A case study of the pilot project in the middle and upper reaches of Fen River in Shanxi Province. *Acta Ecol. Sin.* **2019**, *39*, 8817–8825. [CrossRef]
40. Foga, S.; Scaramuzza, P.L.; Guo, S.; Zhu, Z.; Dilley, R.D.; Beckmann, T.; Schmidt, G.L.; Dwyer, J.L.; Joseph Hughes, M.; Laue, B. Cloud detection algorithm comparison and validation for operational Landsat data products. *Remote Sens. Environ.* **2017**, *194*, 379–390. [CrossRef]
41. Xu, H. A study on information extraction of water body with the modified normalized difference water index (MNDWI). *J. Remote Sens.* **2005**, *9*, 589–595. [CrossRef]
42. Zhang, W.; Du, P.; Guo, S.; Lin, C.; Zheng, H.; Fu, P. Enhanced remote sensing ecological index and ecological environment evaluation in arid area. *Natl. Remote Sens. Bull.* **2022**, *27*, 299–317. [CrossRef]
43. Jiang, L.; Jiapaer, G.; Bao, A.; Guo, H.; Ndayisaba, F. Vegetation dynamics and responses to climate change and human activities in Central Asia. *Sci. Total Environ.* **2017**, *599–600*, 967–980. [CrossRef] [PubMed]
44. Crist, E.P. A TM Tasseled Cap equivalent transformation for reflectance factor data. *Remote Sens. Environ.* **1985**, *17*, 301–306. [CrossRef]
45. Baig, M.H.A.; Zhang, L.; Shuai, T.; Tong, Q. Derivation of a tasselled cap transformation based on Landsat 8 at-satellite reflectance. *Remote Sens. Lett.* **2014**, *5*, 423–431. [CrossRef]
46. Van Nguyen, O.; Kawamura, K.; Trong, D.P.; Gong, Z.; Suwandana, E. Temporal change and its spatial variety on land surface temperature and land use changes in the Red River Delta, Vietnam, using MODIS time-series imagery. *Environ. Monit. Assess.* **2015**, *187*, 464. [CrossRef]
47. Zhang, Y.; Jiang, F. Developing a remote sensing-based ecological index based on improved biophysical features. *J. Appl. Remote Sens.* **2021**, *16*, 012008. [CrossRef]
48. Sen, P.K. Estimates of the Regression Coefficient Based on Kendall's Tau. *J. Am. Stat. Assoc.* **1968**, *63*, 1379–1389. [CrossRef]
49. Partal, T.; Kahya, E. Trend analysis in Turkish precipitation data. *Hydrol. Process.* **2006**, *20*, 2011–2026. [CrossRef]
50. Yang, X.; Meng, F.; Fu, P.; Zhang, Y.; Liu, Y. Spatiotemporal change and driving factors of the Eco-Environment quality in the Yangtze River Basin from 2001 to 2019. *Ecol. Indic.* **2021**, *131*, 108214. [CrossRef]
51. Harka, A.E.; Jilo, N.B.; Behulu, F. Spatial-temporal rainfall trend and variability assessment in the Upper Wabe Shebelle River Basin, Ethiopia: Application of innovative trend analysis method. *J. Hydrol. Reg. Stud.* **2021**, *37*, 100915. [CrossRef]
52. Hurst, H.E. Methods of using long-term storage in reservoirs. *Proc. Inst. Civ. Eng.* **1956**, *5*, 519–543. [CrossRef]
53. Lv, Y.; Xiu, L.; Yao, X.; Yu, Z.; Huang, X. Spatiotemporal evolution and driving factors analysis of the eco-quality in the Lanxi urban agglomeration. *Ecol. Indic.* **2023**, *156*, 111114. [CrossRef]
54. Peng, J.; Liu, Z.; Liu, Y.; Wu, J.; Han, Y. Trend analysis of vegetation dynamics in Qinghai–Tibet Plateau using Hurst Exponent. *Ecol. Indic.* **2012**, *14*, 28–39. [CrossRef]
55. Fan, G.Y.; Cowley, J.M. Auto-correlation analysis of high resolution electron micrographs of near-amorphous thin films. *Ultramicroscopy* **1985**, *17*, 345–355. [CrossRef]
56. Anselin, L.; Syabri, I.; Kho, Y. GeoDa: An Introduction to Spatial Data Analysis. In *Handbook of Applied Spatial Analysis: Software Tools, Methods and Applications*; Fischer, M.M., Getis, A., Eds.; Springer: Berlin/Heidelberg, Germany, 2010; pp. 73–89, ISBN 978-3-642-03647-7.
57. Xue, Z.; Meng, X.; Liu, B. Spatiotemporal evolution and driving factors of ecosystem services in the upper Fenhe watershed, China. *Ecol. Indic.* **2024**, *160*, 111803. [CrossRef]

58. Gong, C.; Lyu, F.; Wang, Y. Spatiotemporal change and drivers of ecosystem quality in the Loess Plateau based on RSEI: A case study of Shanxi, China. *Ecol. Indic.* **2023**, *155*, 111060. [CrossRef]
59. Zhuang, D.; Liu, J. Study on the model of regional differentiation of land use degree in China. *J. Nat. Resour.* **1997**, *12*, 105–111. [CrossRef]
60. Wu, X.; Wang, S.; Fu, B.; Liu, J. Spatial variation and influencing factors of the effectiveness of afforestation in China's Loess Plateau. *Sci. Total Environ.* **2021**, *771*, 144904. [CrossRef]
61. Brunsdon, C.; Fotheringham, A.S.; Charlton, M.E. Geographically Weighted Regression: A Method for Exploring Spatial Nonstationarity. *Geogr. Anal.* **1996**, *28*, 281–298. [CrossRef]
62. Geng, J.; Yu, K.; Xie, Z.; Zhao, G.; Ai, J.; Yang, L.; Yang, H.; Liu, J. Analysis of spatiotemporal variation and drivers of ecological quality in Fuzhou based on RSEI. *Remote Sens.* **2022**, *14*, 4900. [CrossRef]
63. Ma, C.Q.; Yi, Z.Q.; Yuan, X.F.; Zhang, S.M.; Zhang, S.S. Spatial difference of ecological services and its influencing factors under different scales: Taking the Xi' an section of Qinling Mountains as an example. *Res. Soil Water Conserv.* **2024**, *32*, 389–399. [CrossRef]
64. Wang, B.; Fu, S.; Hao, Z.; Zhen, Z. Ecological security pattern based on remote sensing ecological index and circuit theory in the Shanxi section of the Yellow River Basin. *Ecol. Indic.* **2024**, *166*, 112382. [CrossRef]
65. Cao, Y.W.; Yan, J.P. Temporal and spatial analysis of extreme climatic events in Shanxi Province from 1961 to 2013. *Resour. Sci.* **2015**, *37*, 2086–2098.
66. Mi, Z.; Sun, X. Provinces with transitions in industrial structure and energy mix performed best in climate change mitigation in China. *Commun. Earth Environ.* **2021**, *2*, 182. [CrossRef]
67. Zhao, J.; Yang, Y.; Zhao, Q.; Zhao, Z. Effects of ecological restoration projects on changes in land cover: A case study on the Loess Plateau in China. *Sci. Rep.* **2017**, *7*, 44496. [CrossRef]
68. Gao, J.; Zou, C.; Zhang, K.; Xu, M.; Wang, Y. The establishment of Chinese ecological conservation redline and insights into improving international protected areas. *J. Environ. Manag.* **2020**, *264*, 110505. [CrossRef]
69. Sun, H.; Liu, H. The spatiotemporal evolution and improvement path of ecological performance in the Yellow River Basin of Shanxi Province. *Bull. Soil Water Conserv.* **2024**, *44*, 1–15. [CrossRef]
70. Shao, J.; Li, J.; Yan, X.; Ma, T.; Zhang, R. Analysis of spatiotemporal variation characteristics and driving forces of NPP in Shanxi Province from 2000 to 2020 Based on Geodetector. *Environ. Sci.* **2023**, *44*, 312–322. [CrossRef]
71. Li, Q.; Su, Y.; Feng, Z.; Zhou, Z.; Guo, L.; Ma, X.; Liu, G. Study on production-living-ecological space function coupling coordination in Fen river basin. *Sci. Soil. Water Conserv.* **2021**, *19*, 115–125. [CrossRef]
72. Wang, Y.; Liu, C.; Liu, B.; Lee, T.M. Integrated outcomes of large-scale ecological restoration projects on biodiversity–eco-environment–society in China. *Geogr. Sustain.* 2024, *in press*. [CrossRef]
73. Holl, K.D.; Luong, J.C.; Brancalion, P.H.S. Overcoming biotic homogenization in ecological restoration. *Trends Ecol. Evol.* **2022**, *37*, 777–788. [CrossRef] [PubMed]
74. Zhang, Y.; Zhao, X.; Gong, J.; Luo, F.; Pan, Y. Effectiveness and driving mechanism of ecological restoration efforts in China from 2009 to 2019. *Sci. Total Environ.* **2024**, *910*, 168676. [CrossRef] [PubMed]
75. Zhang, X.; Fan, H.; Sun, L.; Liu, W.; Wang, C.; Wu, Z.; Lv, T. Identifying regional eco-environment quality and its influencing factors: A case study of an ecological civilization pilot zone in China. *J. Clean. Prod.* **2024**, *435*, 140308. [CrossRef]
76. Yu, Y.; Zhao, W.; Martinez-Murillo, J.F.; Pereira, P. Loess Plateau: From degradation to restoration. *Sci. Total Environ.* **2020**, *738*, 140206. [CrossRef]
77. Liu, S.; Dong, Y.; McConkey, K.R.; Tran, L.-S.P.; Wang, F.; Liu, H.; Wu, G. Scientific concept and practices of life community of mountains, rivers, forests, farmlands, lakes, grasslands, and deserts in China. *Ambio* **2023**, *52*, 1939–1951. [CrossRef]
78. Liu, E.; Wang, Y.; Chen, W.; Chen, W.; Ning, S. Evaluating the transformation of China's resource-based cities: An integrated sequential weight and TOPSIS approach. *Socio Econ. Plan. Sci.* **2021**, *77*, 101022. [CrossRef]
79. Wen, X.; Zhen, L. Soil erosion control practices in the Chinese Loess Plateau: A systematic review. *Environ. Dev.* **2020**, *34*, 100493. [CrossRef]
80. Tu, C.; Liang, Y.; Fu, Y. How does the environmental attention of local governments affect regional green development? Empirical evidence from local governments in China. *Humanit. Soc. Sci. Commun.* **2024**, *11*, 371. [CrossRef]

Disclaimer/Publisher's Note: The statements, opinions and data contained in all publications are solely those of the individual author(s) and contributor(s) and not of MDPI and/or the editor(s). MDPI and/or the editor(s) disclaim responsibility for any injury to people or property resulting from any ideas, methods, instructions or products referred to in the content.